J Biol Phys
DOI 10.1007/s10867-012-9294-4

ORIGINAL PAPER

Structure-driven homology pairing of chromatin fibers: the role of electrostatics and protein-induced bridging

A. G. Cherstvy · V. B. Teif

Received: 26 September 2012 / Accepted: 11 November 2012

Abstract Chromatin domains formed in vivo are characterized by different types of 3D organization of interconnected nucleosomes and architectural proteins. Here, we quantitatively test a hypothesis that the similarities in the structure of chromatin fibers (which we call "structural homology") can affect their mutual electrostatic and protein-mediated bridging interactions. For example, highly repetitive DNA sequences in heterochromatic regions can position nucleosomes so that preferred inter-nucleosomal distances are preserved on the surfaces of neighboring fibers. On the contrary, the segments of chromatin fiber formed on unrelated DNA sequences have different geometrical parameters and lack structural complementarity pivotal for stable association and cohesion. Furthermore, specific functional elements such as insulator regions, transcription start and termination sites, and replication origins are characterized by strong nucleosome ordering that might induce structure-driven iterations of chromatin fibers. We propose that shape-specific protein-bridging interactions facilitate long-range pairing of chromatin fragments, while for closely-juxtaposed fibers electrostatic forces can in addition yield fine-tuned structure-specific recognition and pairing. These pairing effects can account for some features observed for mitotic and inter-phase chromatins.

Keywords Chromatin pairing · Homology · Electrostatics · Shape recognition · Long-range bridging

A. G. Cherstvy (✉)
Institute for Physics and Astronomy, University of Potsdam,
14476 Potsdam-Golm, Germany
e-mail: a.cherstvy@gmail.com

A. G. Cherstvy
Max Planck Institute for Physics of Complex Systems,
01187 Dresden, Germany

V. B. Teif
German Cancer Research Center (DKFZ) and Bioquant,
69120 Heidelberg, Germany

Published online: 17 January 2013

Abbreviations

FISH|	fluorescence in situ hybridization
ds|	double stranded
bp|	base pair
ES|	electrostatic
PEG|	poly-ethylene-glycol
NCP|	nucleosome core particle
NRL|	nucleosome repeat length
[salt]|	salt concentration
3C|	chromosome conformation capture

1 Introduction

1.1 Electrostatic interactions and protein bridging in homologous DNA pairing

Pairing between homologous chromosomes in meiosis is vital for the reproducible cell division in eukaryotes [1, 2]. During this process, the chromosomal loci with similar (homologous) DNA sequences find each other and zip together into an intimate complex, as monitored, for example in FISH experiments in yeast cells [3–7]. This ensures the correct duplication of chromosomes and their separation between the daughter cells. The degree of this "DNA–DNA intimacy" varies depending on the phase of the cell division, from a maximum of $R > 300$ nm for the most distant DNA–DNA contacts, to $R = 30$–100 nm separation in a synaptonemal complex [8], down to several nm that might be required, e.g., for a successful recombination between the aligned homologous DNAs [9], see Fig. 1. Direct transient DNA–DNA *"kissing interactions"* were proposed to trigger such pairing between homologous ds-DNA fragments. However, the physical nature of forces and their radius of action remain poorly understood. Furthermore, it is still under intense debate how these DNA fragments find their homologous partners so fast and precisely among myriads of non-homologous DNA sequences in a crowded cellular environment [10, 11, 101].

Different physical interactions can contribute at different stages of DNA–DNA pairing. For instance, for two closely juxtaposed homologous DNAs, it has been suggested theoretically that direct DNA–DNA ES forces can yield DNA–DNA zipping [12]. Namely, two homologous DNA fragments aligned at $R = 3$ nm between the axes recognize one another (as compared to non-homologous fragments) with the energy of several k_BT for a DNA length of $L = 300$–$1{,}000$ bp [13], which is on the order of a typical gene length in yeast. This ES recognition is governed in the theory *solely* by the sequence-specific DNA structure that can also provide an impetus for the pairing of homologous DNA fragments in vivo [14].

Indeed, recent experimental studies in dense DNA cholesteric phases under the external osmotic stress of PEG have revealed that in a protein-free environment, DNA fragments of $\sim$300 bp in length are capable of recognizing each other at $R = 3$ nm or $\approx$1 nm between the surfaces [15]. This recognition was demonstrated to be strong and sequence-specific enough to separate DNA fragments into distinct well-defined populations in these dense cholesteric spherulites. This provided the first direct proof of sequence-specific recognition between intact ds-DNA duplexes in vitro. Recent single-molecule DNA pairing experiments have also supported the possibility of DNA–DNA homology pairing [16] in solutions of simple monovalent salt and with apparently looser DNA alignment.

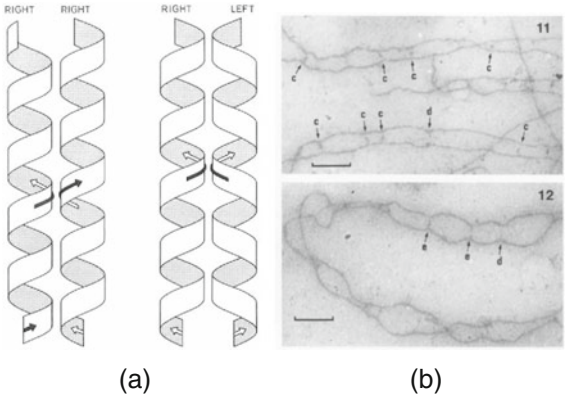

Fig. 1 **a** Schematics of similar- and mirror-symmetric helical ribbons of sister chromatids on metaphase chromosomes. Both structures allow a zipper-like pairing of homologous juxtaposed DNA elements in space (shown by *arrows*) with every helical repeat along the contact. The image is reproduced from [26], with kind permission from Springer Science and Business Media. We implement below a similar model to treat the pairing of homologous chromatin fibers. **b** The formation of synaptonemal complex nodules (indicated by *arrows*), which pair the corresponding sites on homologous chromosomes of *Allium cepa* during zygotene. This image is reprinted from [64], with permission from Elsevier

However, in vivo at initial stages of DNA–DNA homologous pairing in the course of cell division, some distant molecular contacts were shown to be maintained already at ~300 nm between DNA duplexes. In the cytoplasm, with a typical concentration of monovalent salt of $n_0 = 0.1$ M and a Debye screening length of $\lambda_D = 1$ nm, the screened Coulomb ES interactions are only substantial within 1–2 λ_D between the DNA surfaces. Thus, the ES interactions are rendered short-ranged by electrolyte screening. Therefore, these shielded ES forces are unlikely to account for the experimentally reported distant DNA–DNA pairing, as it was shown in Ref. [17]. Here we do not consider direct DNA–DNA ES recognition; instead, we address the recognition of chromatin fibers rather than DNA helices.

Instead, sequence-specific protein-mediated forces between DNAs (involving possibly condensin, cohesin, structure maintenance chromosomal proteins, HP1, CTCF and many other players [18–20]) can establish DNA–DNA contacts and thus expand the radius of action of inter-fiber interactions. In addition, some similarities in the packaging of homologous DNA fragments on a larger scale of the 30 nm chromatin fiber can be involved. Indeed, recent studies have unraveled a number of intermediate classes of chromatin organization [21–23], in addition to earlier views of a chromatin composed of highly condensed heterochromatin and loosely organized euchromatin [24]. These chromatin classes differ dramatically in their physico-chemical properties (NCP density, fiber diameter, etc.) as well as protein composition, concentrations, and gene accessibility [25].

Regular well-ordered heterochromatin fibers are abundant in centromeric and telomeric chromosomal regions. In these domains, the DNA sequence includes a number of highly repetitive elements that might establish some regular structures. This local homology in the DNA sequence yields highly complementary shapes of the regular chromatin fibers for these chromosome regions. Can they recognize the shape similarities analogously to the naked DNA? The problem is that the helical repeat of a solenoidal 30 nm chromatin fiber is of the order of the diameter of the nucleosome, $H = 11$ nm, while the helical pitch of B-DNA is only 3.4 nm. Thus, if complementary interactions between chromatin fibers exist, they would be more long-ranged. Even more questions arise with transcriptionally active,

often irregular, uncondensed euchromatin. Some of these chromatin-pairing issues will be semi-quantitatively discussed below, although we do not exclude that similar mechanisms of pairing can be valid for the recognition of higher-order structures of chromatin [26].

1.2 Interactions between the chromatin fibers

Experimentally, many features of mutual interactions of chromatin fibers remain obscure, partly because of different chromatin forms that can potentially coexist in vivo [27]. Here, one should distinguish between the subtleties in interactions due to the complexity of the internal chromatin structure and due to different biophysical mechanisms likely to be involved. On the theoretical side, the problem of interaction of even regular 30 nm fibers poses a considerable challenge. It stems from a complex fiber structure consisting in inter-wound nucleosome core particles (NCP) with a histone octamer with ∼146–147 bp of DNA wrapped around it, separated by ∼10–60 bp DNA segments and decorated by a number of other chromatin proteins. Locally, the intricate interplay between the opposite charges on DNA and histones totaling to near zero [110] generates moderate ES forces maintaining the chromatin integrity. As we propose below, the pairing efficiency of chromatin fibers is likely to correlate with their geometrical regularity, which is a complex function of a number of parameters. The list includes several structural factors such as the DNA sequence, the length of the linker DNA [111], the presence of linker H1/H5 histones [28], charge modifications of histone tails [29], as well as the environmental factors such as the amount of simple salts and the presence of specific DNA-binding proteins. Positioning of a specific genomic feature, such as enhancer, promoter, noncoding repeat, is another determinant of the type of the chromatin fiber packing.

How the inter-NCP interactions affect the structure of the chromatin and its mechanical properties is still a matter of intense debate. A number of experimental [30–33], theoretical [34–36], and computer simulation studies [37–45] have emerged on this subject in recent years. Chromatin 30-nm fibers interact electrostatically with each other via "contacting" NCPs positioned on the fiber periphery, both in canonical solenoidal [46, 47] and cross-linked [34] fiber models. Several studies were devoted to ES interactions of individual NCPs, including the effects of NCP asymmetry and DNA wrapping geometry [48]. Different strengths of ES forces for the NCP sides with 2 and 1 DNA turns were enumerated [48]. The possibility of NCP-NCP ES cohesion stemming from the DNA–DNA zipper-like ES attraction [49] along the contacting side surfaces of NCPs has been rationalized [50].

One technique to uncover the properties of fiber–fiber interactions in vivo is the 3C [51] and high-C [52] methods. Using these methods, genome-wide maps of probability of contacts between the chromosomal segments have been determined for *Drosophila*, mouse, and human [22, 53, 54]. These maps account for inter- and intra-chromosomal correlations as dictated by DNA–DNA contacts. It has been discovered that more contacts exist between homologous DNA fragments in pre-meiotic cells, as compared to non-homologous DNA loci. This more intimate association of homologs was also detected by the FISH measurements in yeast cells, see e.g., [7]. The 3C data on captured chromosomal conformations for yeast are consistent with the DNA packing density in the chromatin of 6 NCPs per 11 nm along the fiber [51].

De-condensed chromosomes occupy chromosomal territories and, for instance in *Drosophila*, a *non-random* pattern of associations between the territories of homologous chromosomes was discovered [55]. Also, smaller gene-rich active chromosomal domains were shown to exhibit a more frequent homology pairing. In yeast, inactive chromosomal loci were shown to cluster in their corresponding territories, while active segments establish

distant intra- and inter-chromosomal contacts [53]. Note that preferential contacts of heterochromatin-rich domains as well as telomeric and centromeric loci have been identified. This can be caused by a more organized chromatin structure of these regions.

Gene-poor and transcriptionally inactive chromosomal domains occupy the nuclear periphery, often adopting heterochromatin structure [56]. For homologous genes during the S-phase, the phenomenon of *"gene kissing"* has been observed, resulting in a proximal spatial association of genetically distant chromosomal segments. The high-C technique has also revealed that small gene-rich chromosomes prefer to interact with each other and the process is often accompanied by their co-localization in the nucleus center [22].

1.3 Structure of "30 nm" chromatin fibers

Despite numerous experimental and theoretical studies, there is still great concern in the literature about the structure of 30 nm chromatin fibers at different conditions both in vitro and in vivo but at least recent experiments have provided direct evidence that the 30 nm fiber does exist in vivo [21, 32]. Below, we overview several recent studies addressing this issue.

Experimentally, the spatial organization of NCPs in chromatin fibers has recently been unraveled in elaborate fiber reconstitution studies coupled with a cryo-EM visualization [57, 58]. Varying the length of linker DNA between the adjacent NCPs (with the regularly spaced 601 NCP-positioning DNA fragments [112]), the chromatin structures visualized yield the linear density of NCPs and the fiber thickness. Namely, for the linker lengths <60 bp the density of NCPs was $\approx$11 per 11 nm along the fiber, with a fiber diameter of $D \approx 33$ nm. For longer DNA linkers, a step-wise increase of fiber diameter up to $D \approx 44$ nm was shown to occur, with an NCP density of $\approx$15 NCPs per 11 nm. This NCP density is nearly twice as large as the value of 6–7 NCPs per 11 nm assumed in the literature; the fiber diameter is also considerably larger than the canonical value of 30 nm.

The chromatin fiber appears to be strongly *inter-digitated*, with the NCPs on a given helical turn "squeezed" between NCPs in the neighboring turns [57]. A plausible geometrical model of NCP compaction has a period for a simple helix of about $H/2 = 5.5$ nm, because of this dramatic inter-digitation. The fibers were reconstituted at one H5 linker histone per $\approx$200 bp of 601 DNA repeat [57]. This linker histone binds the DNA on its entry and exit points on each NCP, deforming the linker DNA as required for a proper fiber folding. The observations of [57] are consistent with a one-start left-handed solenoid chromatin model [47], rather than with a zig-zag multi-stranded crossed-linked fiber proposed theoretically in [35, 59]. For the latter, the fiber diameter is expected to grow *continuously* with the DNA linker length that was not detected in experiments. Note that in experiments, the fiber structure depends on the concentration of simple salt, with a regular 30 nm fiber often observed only at elevated salinities, whereas an extended 10 nm chromatin is preferred at low-salt conditions [60].

A number of large-scale computer simulations [61, 62] have recently been performed to rationalize the implications of inter-NCP interactions on the structure and stability of chromatin fibers. A large "zoo" of chromatins with various diameters and NCP linear packing densities were produced as a result of these investigations, as a function of model parameters.

Theoretically, some geometrical models of dense packing of wedge-like NCPs on the fiber periphery have recently been proposed [34, 59]. For a proper NCP wedge angle, these authors suggested that multi-stranded 5, 6, 7, and 8 ribbon chromatin fibers can be

realized. It appears that 5- and 7-ribbon chromatins have diameters of $D \approx 33$ and $D \approx 44$ nm, correspondingly, close to the values measured [57] for the corresponding DNA linker lengths. This model also predicts a 6-ribbon fiber with $D = 38$ nm and an 8-ribbon structure with $D = 52$ nm [59], which however have not yet been observed [57]. Although the implications of a continuous DNA inter-connecting the NCPs on different ribbons have not been analyzed in this model [34] and the ES interactions between the components of the system were neglected, so far this is the only theory that discriminates among different chromatin fibers based on the geometrical form of NCPs and elastic properties of wrapped DNA.

In this paper, we do not discuss the physical mechanisms of chromatin fiber formation and higher-order DNA packaging. We rather start with an assumption that local chromatin organization is realized in the structure of a typical 30 nm fiber, as a single- or multi-stranded assembly of inter-connected NCPs. Using this, we discuss some features of fiber–fiber ES and protein-bridging interactions that stem from the fiber geometry. The NCPs on the fiber periphery act as "interaction centers" for both types of forces in the model.

The paper is organized as follows. We start with ES interactions of ideally helical and distorted chromatin fibers, implementing the theory of ES forces between helical macromolecules pioneered by Kornyshev and Leikin in [63] and developed by them in a series of papers together with one of the authors (AGC). Then, we describe a simple equilibrium model for fiber–fiber protein-bridging that also depends on the fiber spatial structure. Finally, we discuss some biological implications and physical limitations of these models.

2 Electrostatic interactions of chromatin fibers

2.1 Ideal helices: models and approximations

The energy of ES interactions of two parallel long ideally helical identical charged fibers of length L can be approximated as the sum of three helical interaction harmonics

$$E(r, R) = L\left[a_0(r, R) - a_1(r, R)\cos\delta\phi + a_2(r, R)\cos 2\delta\phi\right]. \tag{1}$$

In this expression, the coefficients $a_{0,1,2}$ depend on fiber–fiber inter-axial distance R, the structure of the chromatin fiber and the number of helical strands, N_s. All the interaction harmonics a_n are positively defined functions of R and of the fiber radius r. The explicit expressions for single-stranded helical fibers are given via Bessel functions of the second-order K_n as follows (per Å along the fiber–fiber contact)

$$a_0(R) \sim \frac{8\pi^2\overline{\sigma}^2}{\varepsilon}\frac{(1-\theta)^2 K_0(\kappa R)}{\kappa^2\left[K_1(\kappa r)\right]^2},$$

$$a_1(R) \sim \frac{16\pi^2\overline{\sigma}^2}{\varepsilon}\frac{1}{\kappa_1^2}\frac{K_0(\kappa_1 R)}{\left[K_1'(\kappa_1 r)\right]^2},$$

$$a_2(R) \sim \frac{16\pi^2\overline{\sigma}^2}{\varepsilon}\frac{1}{\kappa_2^2}\frac{K_0(\kappa_2 R)}{\left[K_2'(\kappa_2 r)\right]^2} \tag{1a}$$

Here, λ_D is the Debye screening length in the solution, $\varepsilon = 80$ is the solvent dielectric constant, $\kappa_n = \sqrt{1/\lambda_D^2 + (2\pi n/H)^2}$ is the effective reciprocal screening length of the nth harmonic, $H{\sim}110$ Å is the average fiber pitch; $\bar{\sigma}$ is the bare negative surface charge density of the fiber and θ is the fraction of the fiber charge compensated by bound basic histone proteins and counterions adsorbed from the solution (all assumed in the model to be uniformly distributed on the fiber surface).

For the derivation from the linear Poisson-Boltzmann theory, we address the reader to the original papers [49, 63], where the interaction potential between spiral B-DNA duplexes has been derived. For chromatin–chromatin ES interactions, these expressions can be used [63, 65–69]. The only term in a_n that needs to be modified is the so-called "interaction structure factor" f that is responsible for structure-mediated effects [65].

The first term in (1), a_0 provides the energy of ES repulsion of uniformly charged fibers, while the a_1-term describes the helix-mediated force as a function on the mutual azimuthal angle between the fibers, $\delta\phi$. The $a_{1,2}$ terms depend crucially on the helical structure of the fiber. For single-helix, well-separated fibers, the optimal mutual angle is $\delta\phi = 0$ in the model [65]. Often, at biologically relevant conditions, the contribution of the third term in (1) can be neglected, because of a shorter screening length (see below) and smaller magnitude, $a_2 << a_1$. The a_0 term is a function of the fiber charge neutralization fraction θ, $a_0 \propto (1-\theta)^2$, while the harmonics $a_{1,2}$ depend upon the charge pattern on the chromatin fiber.

In the model of Fig. 2, the NCPs are arranged into an ideal spiral of pitch H, while positive charges of histone tails, linker histones, and loosely bound cations from the solution are assumed to be distributed uniformly. For simplicity, we model the helical arrangement of NCP "charge centers" as a continuous thin helix of negative charges (red spirals in Fig. 2). One can incorporate a *finite thickness* of this spiral via a smearing Debye-Waller term in the structure factor that will *diminish* the magnitude of ES interactions [13]. Similarly, the roughness/randomness in the fiber radius $r + \Delta r$ results in the same diminishing factor $\exp\left[-n^2\left(\frac{2\pi}{H}\right)^2 \frac{<\Delta r^2>}{4}\right]$ for the helical harmonics with $n = 1{,}2$, see [65, 70]. Also, each NCP can be treated in the model as a point-like or smeared localized charge, with a magnitude given by the net charge of histone core proteins and wrapped DNA. Therefore, the concepts of the theory of DNA–DNA ES interactions [49, 65] can be implemented here for chromatin–chromatin ES forces.

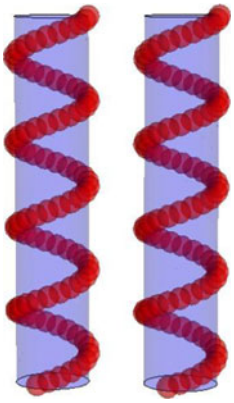

Fig. 2 Schematics of chromatin-chromatin ES interactions, with a positive-negative charge zipper along the fiber–fiber contact. In the model, a continuous spiral of negative charges represents a super-helix of NCPs (in *red*) and a uniform positively charged fiber "background" mimics the histone tails, linker histones, and weakly bound DNA counterions (in *blue*)

The variation of interaction coefficients with the radius of a one-start helical chromatin fiber is illustrated in Fig. 3. A typical value for the fiber pitch $H = 110$ Å was used to represent a dense axial packing of NCPs. In this plot, the fiber surface charge density corresponds to a single-spiral chromatin with ≈7 NCPs per helical turn of 11 nm, each NCP with ≈ 50 negative elementary charges e_0. This value is a realistic estimate for the extent of NCP overcharging by a poly-anionic ≈150 bp long DNA fragment wrapped around the histone core (namely, $\sim +200 \div 250$ e_0 charges on the core and ~ -300 e_0 on the DNA [71–73]). As compared to DNA–DNA ES forces (see Fig. 1 in [68]), for a fiber radius of $r = 15$ nm, the interaction harmonics are much larger because of a larger contact area and a higher linear charge density of chromatin fibers. As expected, the interaction harmonics decay nearly exponentially with the fiber–fiber distance, see Fig. 3.

ES attraction between chromatin segments is realized when $\partial E/\partial R > 0$. This attractive branch of the potential is often accompanied by the condition $a_1 > a_0 + a_2$ for the interaction harmonics. Such attraction between net similarly charged helices occurs via the *charge zipper* mechanism pioneered for the two ideally helical DNA duplexes in [49] and due to the same physical nature for chromatin fibers. Namely, at a proper azimuthal alignment of $\delta\phi = 0$, a negative NCP-rich region on one chromatin fiber faces a positively charged NCP-poor "patch" on the neighboring fiber (see Fig. 2). This short-ranged structure-induced charge matching, described for helices by a_1 term in (1) [14], can overwhelm the Debye-Hückel ES repulsion inevitable for net-charged objects (the a_0 term). The interaction energy for ideal helices of length L is then

$$(a_0 - a_1 + a_2)\, L.$$

For single-stranded helices, one can often neglect the a_2-term in (1).

Since $a_0 \propto (1-\theta)^2$, the region of fiber–fiber attraction is the widest at $\theta = 1$ for fully neutralized fibers. As the fraction θ is not well known, in Fig. 4 we present the phase diagram of fiber–fiber attraction as obtained from this ES model for varying θ. It illustrates that the region of strongest attraction mediated by helix–helix ES cohesion is located in the region when the fiber–fiber distance is $\sim \lambda_D$. The attraction–repulsion transition curves (thick curve) for the fibers of different diameters (e.g., 20, 30, and 40 nm) almost superimpose (not shown). Figure 4 also illustrates that a minimal θ value is required to

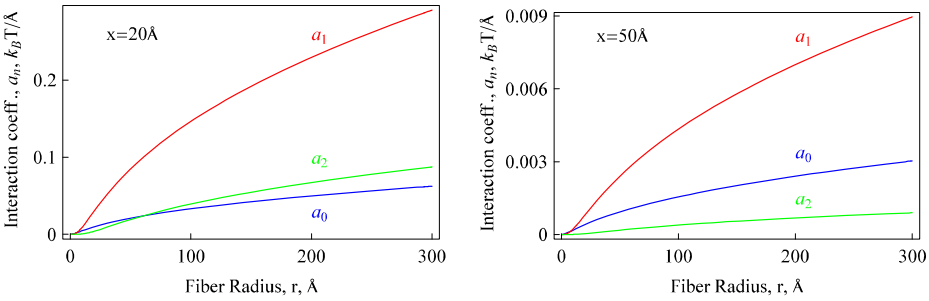

Fig. 3 The fiber–fiber ES interaction for single-stranded chromatin helices in close contact. Parameters: the fiber surface-to-surface separation is $x = 20$ Å for the left and $x = 50$ Å for the right graph, the chromatin is 50% neutralized, $\theta = 0.5$, the fiber net negative charge density is 1 e_0/300 Å^2, the helix pitch is $H = 110$ Å and the Debye length is $\lambda_D = 10$ Å

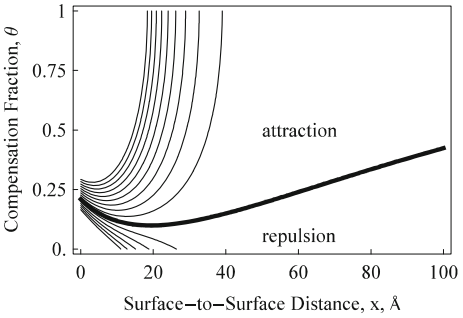

Fig. 4 Inter-chromatin attraction-repulsion diagram for varying fiber–fiber distance $R = 2r + x$ and its neutralization fraction θ. Parameters: fiber radius is $r = 15$ nm, other parameters are the same as in Fig. 3. Equidistant energy contours are shown on both sides of the attraction–repulsion transition (thick curve)

trigger the attraction, when fiber surfaces are just 1–2 $\sim\lambda_D$ away from each other. Helix–helix ES zipper attraction is the strongest in this region [50].

2.2 Non-ideal helices

In analogy to DNA–DNA ES forces [13, 65], one can envisage the effects of *fiber non-ideality* on the strength of inter-chromatin interactions. The fibers are assumed to be always straight and these non-idealities are related to the helical symmetry. Namely, for non-ideally-helical chromatin fibers the positive-negative charge register cannot persist infinitely long along the fiber axis. The distortions of fiber helicity can be of random nature (randomness in DNA linker length, variation of fiber thickness, thermal fluctuations, etc., see Discussion section) or they can be mediated by structural non-commensuration of the chromatin (e.g., the fibers with different values of helical pitch or number of helical strands). Randomly distorted chromatin fibers will interact weaker and even at best conditions might not yield fiber–fiber cohesion.

However, if the fibers have a small enough twist persistence length,

$$l_{tw} = k_B T C,$$

these non-similarities in the helical structure can be reduced via the torsional adaptation of fibers. As a result, a zipper-like charge matching along the fibers is largely restored, allowing for ES fiber–fiber pairing (See [13] where the mathematical analysis of this effect was developed for non-ideal DNA duplexes). For the second type of "regular" fiber distortions, the exact analysis will not be considered here. Generally, the fibers with the helical repeats that are multiples of one another can still *lock in register* and exhibit cohesive ES forces, as dictated by the symmetry laws found for helix–helix interactions [83].

For long fibers with *random* distortions of NCP positions from a helical symmetry and in the absence of torsional adjustment (rigid fibers), a simple result can be derived. In this limit, the magnitude of helical terms $a_{1,2}$ decays after some fiber length longer than the so-called *correlation length* of structural variations, λ_c [12, 14]. The more irregular the helices are, the shorter this length is going to be. The interaction energy is then solely defined by the Debye-Hückel repulsion of homogeneously charged rods, which is $a_0 L$ for long helices with $L >> \lambda_c$. Then, the ES recognition energy ΔE between the two homologous and two structurally distorted chromatin fibers is (in the limit $a_2 << a_1$)

$$\Delta E_{rigid} \approx a_1 L - a_1 \lambda_c, \tag{2}$$

in analogy to DNA–DNA sequence recognition [12, 13]. The values of a_1 can be extracted from Fig. 3. For relatively short interacting fragments, the full expression for the non-linear growth of the recognition energy is

$$\Delta E_{rigid} = a_1 \lambda_c \left\{ \frac{L}{\lambda_c} + \exp\left[-\frac{L}{\lambda_c} \right] - 1 \right\}, \tag{2a}$$

see [12, 13, 74] for details and Fig. 5.

For two non-homologous fibers with easy torsional adaptation (soft fibers), the linear dependence with the fragment length L in (2) survives for long fragments, while the pre-factor is renormalized. It is multiplied by a small ratio of the torsional adjustment length $\lambda_t = \sqrt{C/(2a_1)}$ to the correlation length λ_c that yields for the recognition energy [68, 74]

$$\Delta E_{soft} \approx a_1 L \frac{\lambda_t}{2\lambda_c} - \frac{a_1 \lambda_t^2}{4\lambda_c}. \tag{2b}$$

Again, for relatively short interacting fragments, the full expression is [74]

$$\Delta E_{soft} = a_1 L \frac{\lambda_t}{2\lambda_c} - \frac{a_1 \lambda_t^2}{4\lambda_c} \left\{ 1 - \exp\left[-\frac{2L}{\lambda_t} \right] \right\}. \tag{2c}$$

All these four recognition energy expressions are plotted in Fig. 5. For long sequences, the energies grow linearly with the length of interacting chromatin fragments L, while for short fragments, the exact energy expressions above reveal a quadratic increase,

$$\Delta E_{rigid}\,(L \to 0) = \Delta E_{soft}\,(L \to 0) \approx \frac{a_1 L^2}{2\lambda_c}.$$

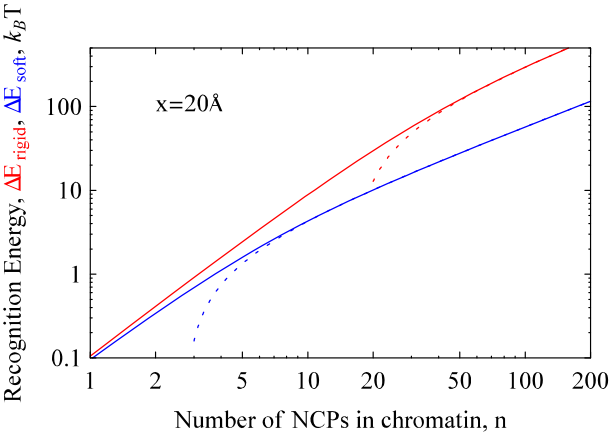

Fig. 5 ES recognition energy for torsionally rigid (*red curve*) and torsionally soft (*blue curve*) chromatin fibers. The *dotted curves* are plotted according to (2) and (2b), while the *solid curves* are the full expressions for the recognition energy, (2a) and (2c). The chromatin fiber contains $n = 6$ NCPs per helical repeat of 110 Å for the one-stranded helix, i.e., for this canonical solenoidal fiber $L = 110n/6$. Parameters are the same as in Fig. 3, the fiber diameter is 30 nm and the surface-to-surface distance is $x = 20$ Å

Using the values of a_1 from Fig. 3, the fiber torsional rigidity modulus C (which is unfortunately poorly known [75, 76]) and the length of interacting fragments, one can assess the strength of the resulting recognition. If it is much larger than the energy of thermal agitation, at close distances the ES recognition can trigger the association of homologous chromatin loci in favor of non-homologous ones. Of course, for more separated chromatin fibers, the ES recognition energy both for rigid and soft fibers decreases nearly as

$$\propto \exp\left[-x/\lambda_D\right]$$

due to the Debye-Hückel screening of a_1. For instance, the magnitude of ΔE drops about 30 times as we go from 20 to 50 Å separations between the fiber surfaces, see Fig. 3.

As one can see from Fig. 3, even for uniformly distributed counterions, the fiber–fiber ES attraction is possible in the model. Its magnitude can be enhanced via a proper distribution of counter-charges on the fiber, so that the positive-negative charge alternation in the ES zipper is maximized. In analogy to DNA, where the counterions can adsorb in the DNA helical grooves, for chromatin fibers, the positive charges positioned as helical strands *in-between* the strands of negative charges representing the NCP-strands might facilitate the ES attraction (not shown). There is, however, no experimental evidence that such a charge pattern is relevant, so we keep a uniformly charged fiber background as a more realistic scenario.

One immediate conclusion of this linear Poisson-Boltzmann theory is the estimate of the value of the radius of action of inter-chromatin ES forces. In the presence of simple salt in the solution at concentration n_0, this range is given for the uniformly charged objects by the Debye length,

$$\lambda_D = 1/\sqrt{8\pi l_B n_0}.$$

The latter is $\lambda_D \approx 10$ Å at a physiological amount of simple salt ~0.1 M. For helix–helix ES interactions, this length is being modified by the spiral structure of the molecule and for the two single-stranded helices the screening length is [14, 63]

$$\kappa_1 = 1/\lambda_1 = \sqrt{1/\lambda_D^2 + (2\pi/H)^2}. \tag{3}$$

Thus, the chromatin helices with a larger helical pitch H have a somewhat longer screening length of ES helix–helix interactions, which can be an experimentally testable prediction. However, this decay length is always shorter than the Debye length. In the absence of salt, the helix geometry alone defines the interaction range and $\lambda_1 = H/2\pi$.

2.3 Multi-stranded helices

The situation is more complicated for multi-stranded helical fibers. The screening length then depends on the number of equidistant strands N_s as follows [63]

$$\kappa_1 = \sqrt{1/\lambda_D^2 + \left(2\pi N_s/H\right)^2}. \tag{4}$$

Therefore, in low-salt solutions (see the estimates below), multi-stranded fibers exhibit a *stronger* shielding of helix-specific interactions, with $\lambda_1 = H/(2\pi N_s)$. So, the ES helix-specific forces are screened better for multi-stranded fibers (at the same charge density, fiber

diameter, and inter-fiber distances). This might suggest a way to probe the fiber structure based on the radius of action of chromatin–chromatin ES forces.

The interaction coefficients are also non-trivial functions of N_s. Namely, for N_s equidistant helical strands forming a hyper-spiral structure, the symmetry demands that the system remains equivalent upon a multiple of $2\pi/N_s$ azimuthal rotation of the fiber. This yields that only the a_n terms with $n = jN_s$ will survive [77]. So, for the two-stranded chromatin helix $a_{n=1,3,5,...}$ are identically zero and the leading helical term is a_2. For the equidistant triplex and quadruplex fibers, the leading helical terms are a_3 and a_4, correspondingly and typically $a_{3,4} << a_1$.

All in all, we expect that shorter decay lengths and weaker helical harmonics render the ES interaction of multi-stranded helical fibers measurably weaker than for single-stranded helices. The physical reason is that these multi-stranded fibers bear a *weaker charge alternation* along the fiber and thus a zipper-driven fiber–fiber ES attraction is diminished. This can be tested in experiments, if ES forces indeed govern the association of closely juxtaposed chromatin fibers. To make this attraction possible, the fibers have to align locally at an optimal azimuthal orientation (that is $\delta\phi = 0$ for well-separated fibers [63]).

Note that depending on the number of NCP ribbons in the fiber and its helical pitch, there exists a critical salt concentration below which the structure-mediated screening dominates over the Debye screening. For example, using (3) and (4), for B-DNA with a pitch of 34 Å this critical [salt] is ≈300 mM. For one-start chromatin spirals with $H = 110$ Å it is $c_1 \approx 30$ mM, while for a two-start fiber with the same H it is $c_2 \approx 100$ mM of simple salt. In principle, performing experiments in buffers at salt concentrations much lower than the critical values $c_{1,2}$ one can monitor the dependence of fiber–fiber ES forces on fiber structure. This might give a clue about the strandedness of chromatin fibers under investigation. At higher salinities, these structure-mediated effects are masked by Debye screening. Note that the values $c_{1,2}$ are somewhat lower than the physiologically relevant values, so these fine features of chromatin–chromatin forces are not expected to be pronounced in a typical nuclear environment.

The main message of this chapter is that at physiological $\lambda_D = 10$ Å the ES fiber–fiber interactions are very *short-ranged*. Although our DNA-inspired model for inter-chromatin interactions does predict a fiber pairing, the radius of action of these forces is too small. We need to invoke another mechanism of chromatin pairing that can potentially have a larger range, involving protein-mediated bridging of aligned chromatin fibers, as discussed below.

2.4 Limitations of the ES model

2.4.1 Irregularities of the DNA repeat length

The DNA linker length between neighboring NCPs along a genomic DNA is known to be quantized with a period of DNA helical repeat of 10–10.5 bp [78]. This provides an element of irregularity in the chromatin structure. Similarly to DNA, the implications of this randomness onto fiber–fiber interactions can be rationalized via the introduction of a random field of NCP displacements, if they are small. Indeed, typical $\pm n$*10-bp DNA linker length variations (usually $n = 1, 2, 3$) can be considered small as compared to about 1,200 bp of DNA per one helical turn in the chromatin fiber (ca. 6–7 NCPs with ≈200 DNA bp each). Note, however, that fiber irregularities induced by these variations can vary for different nucleosome repeat lengths, NRL. For instance, in yeast *S. pombe*, this repeat length is only $NRL = 165$ bp [79], while the sperm of sea urchin *A. punctulata* has $NRL = 260$ bp

[80]. Furthermore, the NRL charges for different genomic regions of the same cell [81] and it is altered in the course of cell differentiation [82].

2.4.2 Thermal bending fluctuations of chromatin

At biologically relevant fiber–fiber separations, chromatin thermal undulations are expected to smear the helix-mediated ES pairing of homologous fibers. However, for very close contacts, the opposite situation can be realized because of enhanced close-range image forces, like for DNAs [69].

2.4.3 The discreteness of NCP charges

In the ES model above, the NCP ribbons were treated as continuous charged spirals. The effect of NCP charge discreteness, in addition to the zipper effect due to charge alternation along the fiber axis, give rise to a more delicate effect of charge ordering along the spiral. One can expect here that, similarly to DNA–DNA forces [83, 84], an *integer number* of NCPs per helical turn in a fiber will be preferred. For the naked DNA, an over-winding from 10.5 in dilute solutions to 10.0 bp/turn has been observed experimentally in dense hydrated DNA "fibers". In the ES model, this is triggered by more favorable interactions between the 10.0 bp/turn DNAs. For such an arrangement, intermolecular interactions may be fine-tuned via forming ridges of phosphate charges parallel to the DNA axis. Matching these ridges with the fine grooves of more positive charges on a neighboring DNA yields a lower ES energy for an integer number of bp per turn [83]. This ridge-groove matching is established via a proper azimuthal adjustment of discretely charged spirals. Likewise for the chromatin, the *discrete NCPs will form ridges along the fiber axis* and each NCP on the ridge will face a NCP-free more positive patch on the aligned groove on the neighboring fiber. A similar fine-tuning effect might occur also for protein-bridging interactions (see below).

3 Protein bridging fiber–fiber interactions

3.1 Chromatin pairing and structural homology

Protein-induced bridging of neighboring or distant DNA regions is a well-known phenomenon [85, 86]. One specific example that recently appeared in the focus of the biophysical community is CTCF proteins [21, 87–90]. Several thousands of CTCF binding sites have been identified in human and mouse chromatin. Interestingly, these sites are cell-type dependent [89]. Many sites of CTCF proteins act as boundary elements, separating chromatin regions into active and inactive states [90]. At these sites, a single bound CTCF protein positions up to 20 NCPs in its vicinity in a quite regular order [88]. Most of these ordered nucleosomal arrays are characterized by NCP-depleted regions surrounding the CTCF site, followed by the oscillations of the probability to find a NCP at separations n^*NRL, where n is an integer number.

CTCF proteins are known to demarcate the boundaries of hetero- and eu-chromatins by looping distant chromatin regions [22]. Genome-wide 3C and CTCF binding maps revealed that the binding sites for cohesin are often co-localized with those for CTCF proteins and some DNA loci require cohesion to establish CTCF-mediated inter-chromatin contacts [14].

If a regular nucleosome pattern is present on both sides of the CTCF-mediated bridge connecting two NCP arrays, then these two nucleosomal arrays are likely to exhibit a *structural homology*. As a result, the NCPs on one array are positioned in front of NCPs or NCP-"holes" on the second array. This well-defined arrangement of NCPs can provide the source of shape-specific recognition of chromatin fibers, as described below.

3.2 A model of protein-induced chromatin bridging

In this section, we describe a physical model of chromatin pairing based on sequence-specific protein-mediated fiber–fiber bridging. The problem of polymer- and protein-mediated bridging forces between two rod-like fibers has been investigated in a number of theoretical [91–94] and computer simulation [95, 96] studies. None of these models, to the best of our knowledge, has treated the effect of substrate homology and chromatin shape recognition.

In particular, in [91] the bundling transition of semi-flexible uniformly charged biopolymer chains in the presence of cohesive linkages has been analyzed theoretically and supported by computer simulations. It has been revealed, e.g., that above a critical density of linkers bound simultaneously to two chains the inter-chain interaction is rendered attractive, overwhelming the inter-chain Debye-Hückel ES repulsion and chain bending energy. The maximal density of linkers is realized for parallel chains, while in this state chain–chain ES repulsion is also maximal. The undulatory chain profiles with periodically bound linkers were predicted at a small density of associated bundling proteins.

In the opposite limit of high linker density, some aggregated *railway-like* paired chain configurations coupled by densely bound linkers were predicted, as the energy-optimal state via minimization of the sum of linker-chain binding, chain bending and inter-chain ES repulsion energies. One example of these "generalized linkers" features multivalent cations that are capable to bridge negatively charged DNAs from solution into dense condensates. Also, in [92] the model of DNA condensation in the presence of multivalent chain-like polyamines based on cooperative ligand binding has been proposed and compared with experimental data.

In our model, two juxtaposed regular chromatin fibers can be bridged together by protein linkers, which are characterized by the binding affinity to a set of interaction sites determined by the fiber structure. This binding affinity, the linear density of binding sites and concentration of free linkers in solution are the model parameters that control fiber pairing. For homologous fibers bridged by linkers, the pairing takes place above some critical values of the binding strength and the density of linkers bound to aligned fibers. For non-homologous fibers, such a bridging necessitates also elastic deformations of linkers or the fibers that then constitute the recognition energy, ΔE.

One essential difference between the direct ES and protein-bridging interactions is the optimal azimuthal phase of aligned fibers. This angle for N_s-stranded helices is 0 for ES zipper-like forces and $2\pi/(2N_s)$ for protein-bridging forces. The latter are optimized when the two helical strands of NCPs oppose one another on the aligned fibers, because they are then "stitched" together by linkers with positively charged DNA-binding domains (see Fig. 6).

The main purpose of the simple model proposed below is to mimic how the *degree of plasticity* of protein linkers can facilitate bridging two chromatin fibers with some degree of non-homology, δ. Since we model the chromatin fibers as regular 1D arrays of interaction centers, this parameter scales with the difference in helical repeats, $\delta = \frac{H_1 - H_2}{H_1 + H_2}$, where

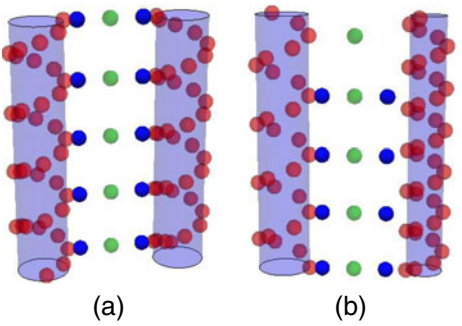

Fig. 6 Schematics of protein bridging pairing of single-helix homologous (**a**) and non-homologous (**b**) chromatin fibers. Homologous fibers are azimuthally rotated by π yielding optimal bridging propensity for the linkers. Non-homologous fibers (**b**) necessitate elastic deformations of linkers that weaken attractive bridging. The NCPs are shown as *red spheres*, with a negative charge. The fiber core is the *bluish rod* with an overall positive charge due to histone tails and linker histones. Identical fibers permit pairing with minimal elastic deformations of linkers. Positively charged domains of the linkers are shown as *blue spheres* bound to NCPs, while a flexible protein hinge is shown as a *green sphere*

$H_1 > H_2$. Neglecting the helical symmetry of the fibers, in a simple 1D case, the elastic energy of linker deformations for the binding of n sites along the fibers with different helical repeats is

$$E^n_{el} = \sum_{j=0}^{n-1} \frac{k}{2} \left[\sqrt{(j(H_1 - H_2))^2 + R^2} - R_0 \right]^2, \tag{5}$$

where k is the elastic stretching modulus of protein linkers and R_o is the equilibrium separation between the chromatin-binding domains of the linker (see Fig. 7). This energy is always larger than the elastic energy penalty to pair two homologous fibers, which is just $E^n_{el,0} = n\frac{k}{2}[R - R_0]^2$.

For small n, the fibers are only slightly non-commensurate and the recognition energy starts accumulating from zero. After a number of sites, as the elastic energy penalty in (5) accumulates, at the site $\bar{n}$ it exceeds gain in the linker-NCP binding energy, $E^{\bar{n}}_{el} > |E_b|$. In this case, an unbound interaction center appears and a kink-like deformation takes place,

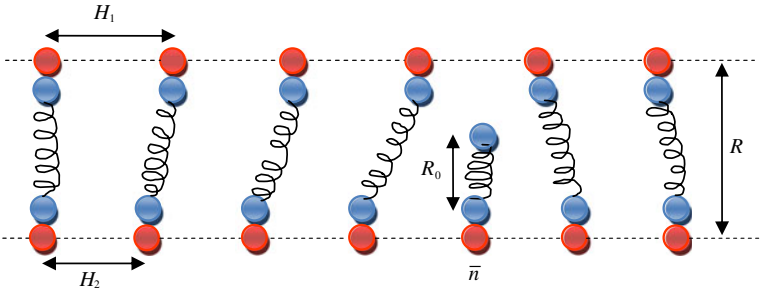

Fig. 7 Schematic 1D model of linker-induced fiber bridging and kink formation. Again, the negatively charged NCPs are shown as *red circles*, while positively charged domains of NCP bridging proteins are depicted as *blue circles*

relaxing this progressive elastic energy build up. The recognition energy of two homologous vs. non-homologous fibers with n bridged nucleosomes is

$$\Delta E(n) = \sum_{j=0}^{n-1} \frac{k}{2} \left[\sqrt{(j(H_1 - H_2))^2 + R^2} - R_0 \right]^2 - n \frac{k}{2} [R - R_0]^2 > 0. \quad (6)$$

Once the site $\overline{n}$ is reached, the fibers become commensurate again and the elastic energy after this grows much slower. This happens at the expense of one missing binding energy and one elastic connection that need not be formed. So, at the site $\overline{n}$ the energy $|E_b| - \frac{k}{2}(R - R_0)^2$ is to be added to the recognition energy $\Delta E(\overline{n})$. This gives rise to an *abrupt jump* in the graph on Fig. 8 and this "penalty" situation repeats every time this critical elastic energy is accumulated. Of course, some additional flexibility of the fibers can reduce the magnitude of these jumps in the recognition energy.

As the linker-NCP binding energy decreases, the energy of elastic deformations exceeds $|E_b|$ after a smaller number of paired NCPs, compare the blue and red curves in Fig. 8 for -10 and $-5\ k_B T$, respectively. As a consequence, the slope of the recognition energy growth with the length of bridged fibers decreases for weaker binding energies. Also, as the fibers become more dissimilar, this critical number of paired centers is achieved earlier and the kinks are more frequent (compare the blue and green curves in Fig. 8 for $H_1 - H_2 = 2$Å and 5 Å, respectively, plotted at the same value of the binding energy).

Such a complementarity recognition model for chromatin fibers is reminiscent of the model of protein-DNA ES recognition proposed in [97]. The main distinction is that here the parameter δ is not necessarily small and a kink formation is possible. Such kinks remind us of the Frenkel-Kontorova model of an elastic chain of inter-connected beads in a non-commensurate sin-like potential [98, 99]. Note also that a closely related model of relaxation of mismatches via twist kink formation has been developed for torsional adaptation of non-homologous DNAs [100] (compare Fig. 13b in this reference with Fig. 8 below).

Note also that in a more advanced model, in analogy to DNA–DNA ES recognition, one can implement a quasi-random variation of the helical repeats on interacting chromatin fibers. This would diminish the accumulation of mismatches in NCP position with the length of fragments in contact (from a ballistic rule for constant incommensuration for $H_1 \neq H_2$ to a diffusive one for random variation in the fiber pitch). So, longer fragments will be required to create a non-commensuration kink on intimately paired chromatin fibers of this kind.

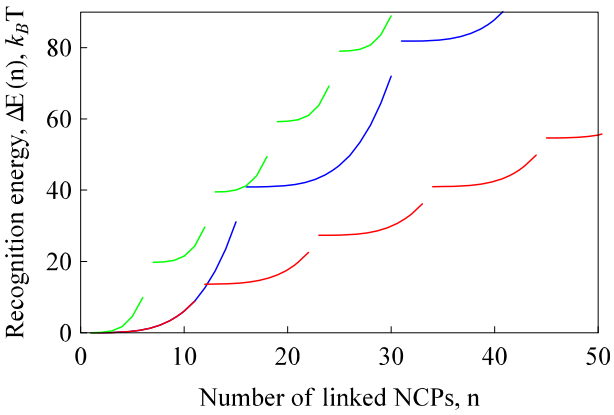

Fig. 8 The recognition energy of protein-bridging interactions for regular chromatin fibers with different helical pitches. Parameters: $k = 0.1 k_B T/\text{Å}^2$, $H_2 = 100$ Å, $R_0 = 30$ Å, $R = 32$ Å; $H_1 = 112$ Å and $E_b = -10 k_B T$ for the *blue curve*, $H_1 = 112$ Å and $E_b = -5 k_B T$ for the *red curve* and $H_1 = 115$ Å and $E_b = -10 k_B T$ for the *green curve*

3.3 Limitations of the protein bridging model

3.3.1 Single- vs. multi-stranded fibers

One problem is to describe the helix of NCPs on the fiber periphery by a unique helical pitch H and a number of NCPs per turn n. The structure of chromatin fibers can be assumed to be inter-digitated, with NCPs on a given helical turn along the fiber squeezed in-between NCPs in the neighboring turns [57]. The geometrical model was suggested with a helix period equal to a half of the NCP diameter, $110/2 = 55$ Å. Such a NCP arrangement can allow for multi-stranded helical representations of the fiber, with different H and n values. The interaction energy will then be the function of the NCP density along the fiber and fiber thickness.

3.3.2 Temperature and fluctuation effects

In the model above, zero-temperature limit and non-fluctuating fibers are considered. Intuitively, one expects that complementarity matching of fibers is impeded by thermal fluctuations but for non-completely matched fibers it is not always the case. Thermal agitation of such fibers might actually help them to recognize each other! This counter-intuitive statement is only valid in a limited T range, where the enhanced fluctuations of interaction "centers" might facilitate the overlap of the corresponding structure factors [102], making the fibers more homologous. At higher T, large fluctuations of the surface groups entirely destroy the complementarity of two interacting surfaces and no pairing is possible.

4 Discussion and conclusions

We have quantitatively evaluated a hypothesis that neighboring chromatin fibers can sense the structure homology determined by the mutual arrangement of nucleosomes. To address this issue, we have considered two conceptually different possibilities: 1) The chromatin fiber structure induces ES forces that allow short-range ES recognition between the structurally homologous surfaces. 2) The chromatin fiber structure modulates protein-induced DNA bridging in such a way that bridging structurally homologous chromatin segments becomes energetically favorable.

For the first case, we have shown that complementary fibers might be *locked in a charge register* that will induce their pairing into an intimate and stable complex. However, these ES forces have a very short-range, with the radius of action not exceeding 1–2 Debye lengths (∼1–2 nm for relevant situations in vivo). For torsionally-soft non-homologous fibers, such pairing is still possible due to a torsional adaptation of the chromatin. Linear deformations of the NCP arrays considered in this 1D model can be mapped onto twist deformations of real chromatin fibers. We have discussed how the screening length of fiber–fiber ES forces depends upon the number of NCP strands and the pitch of the chromatin helix.

In the second case, we implemented a 1D protein-bridging chromatin model that might yield forces of a longer range, which become relevant for chromatin pairing at higher dilutions, as observed experimentally. In this setup, the deformations of elastic protein linkers play the role of chromatin torsional adaptation in the first part of the paper. The

fiber–fiber recognition energy computed reveals a *kink-like adaptation* due to a non-linear accumulation of the elastic energy necessary for successful chromatin bridging by proteins. This non-linear accumulation of mismatch is qualitatively similar to that in the ES model; it stems, however, from regular differences in the helical repeats of the fibers $H_{1,2}$. It would be interesting to test these predictions for experimentally characterized protein-induced chromatin bridges that orderly position several nucleosomes in their vicinity, such as e.g., CTCF insulator proteins.

Our results on pairing of chromatin fibers via shape similarities can also provide new insights on DNA–DNA contact probabilities data for de-condensed chromatins. Of course, the models proposed above are limited to the equilibrium situation, while the pairing observed in vivo and in vitro might also involve some non-equilibrium, dynamical issues.

A recent in vitro study showed that short fiber stretches containing several nucleosomes, extracted from chromatin by mild MNase digestion, readily form ordered structures in vitro, indicating that chromatin fibers do sense the shapes of each other [103]. In addition, our modeling suggests that chromatin fibers not only sense the general shapes but can also distinguish in- and out-of-register arrangements of nucleosomes, suggesting interplay of recognition mechanisms on different length-scales.

The idea of long-range chromatin interactions mediated by protein linkers is currently well accepted [46, 47]. In addition, some non-specific long-range attractive interactions between the chromatin fibers are expected to be triggered by macro-molecular crowding by proteins, RNA, etc. [11, 104–106]. In many prokaryotes, such components can occupy up to 30% of the cell volume thereby inducing attractive depletion-like forces between the interacting DNAs [86]. The theory also predicts that super-coiling can facilitate non-specific pairing of DNAs and chromatin fibers [107]. Such non-specific chromatin attraction might allow to overcome the repulsive ES potential between the fibers, bringing them into a closer juxtaposition, where fine-tuned structure-homology attraction might come into play. The implications of additional non-specific chromatin compaction due to a sub-diffusive behavior of telomeres [108] and the existence of well-defined chromosomal territories [109] onto chromatin-chromatin recognition also remains to be understood.

Chromatin exists in a number of states depending on the cell cycle. For mitotic chromosomes, our model scales up the previous concept of fiber–fiber recognition due to sequence homology and introduces a new notion of structural homology. In this new model, the elementary lattice unit of the DNA double helix (base pair) is substituted by the elementary lattice unit of the chromatin fiber (nucleosome). In both cases, lattice units of the neighboring lattices can be still arranged in- and out-of-register and thus conceptually explain the recognition of the homologous parts of chromosomes. In addition, our model provides a simple and appealing explanation for the formation of chromatin domains in the inter-phase chromatin. In this case, there is no sequence homology but the structural homology is due to the similar arrangements of nucleosomes along the DNA at certain functional elements (e.g., centromeric, pericentric, telomeric, and insulatory chromatin regions). It remains to be verified whether these theoretically predicted effects realize *in vivo* and whether they have a significant role in genome functioning.

After this paper was accepted, we became aware of the experimental study [113]. The authors have confirmed that selective associations between NCPs with identical DNA sequences do reveal a higher propensity of NCP formation, both for free NCPs in solution and DNA-linked chromatin-like NCP arrays. Although the mechanisms underlying the recognition and assembly of homologous and non-homologous DNAs and NCPs need not

be absolutely identical, both require Mg^{2+} cations (10 mM Tris buffer with up to 1 mM of MgCl2 [113]). These Mg^{2+} cations systematically favor a globular condensed state of NCPs, both for the octamers of NCPs with 601 and 5S DNA sequences, as well as for the chimera mixings of these. These DNA-driven NCP-NCP associations prove the possibility of homology recognition not only for straight DNA fragments, as in Ref. [15], but also for strongly curved, biologically relevant DNA conformations in chromatin-like NCP structures, supporting the homology model developed in the current paper.

Acknowledgements Stimulating discussions and correspondence with N. Kleckner, M. Prentiss, and K. Rippe are gratefully acknowledged. AGC acknowledges support by the Deutsche Forschungsgemeinschaft, DFG Grant CH 707/5–1 to ACG. VBT was supported by the DKFZ Intramural Grant and the fellowship of the Heidelberg Center for Modelling and Simulation in the Biosciences (BIOMS). Insightful comments of an anonymous referee are particularly acknowledged.

References

1. Kleckner, N.: Meiosis: How could it work? Proc. Natl. Acad. Sci. U. S. A. **93**, 8167–8174 (1996)
2. Storlazzi, A., Gargano, S., Ruprich-Robert, G., Falque, M., David, M., Kleckner, N., Zickler, D.: Recombination proteins mediate meiotic spatial chromosome organization and pairing. Cell **141**, 94–106 (2010)
3. Kleckner, N., Weiner, B.M.: Potential advantages of unstable interactions for pairing of chromosomes in meiotic, somatic, and premeiotic cells. Cold Spring Harbor Symp. Quant. Biol. **LVIII**, 553–565 (1993)
4. Weiner, B.M., Kleckner, N.: Chromosome pairing via multiple interstitial interactions before and during meiosis in yeast. Cell **77**, 977–991 (1994)
5. Burgess, S.M., Kleckner, N., Weiner, B.M.: Somatic pairing of homologs in budding yeast: existence and modulation. Genes Dev. **13**, 1627–1641 (1999)
6. Zickler, D.: From early homologue recognition to synaptonemal complex formation. Chromosoma **115**, 158–174 (2006)
7. Burgess, S.M.: Homologous chromosome associations and nuclear order in meiotic and mitotically dividing cells of budding yeast. Adv. Genet. **46**, 49–90 (2002)
8. Kleckner, N.: Chiasma formation: chromatin/axis interplay and the role(s) of the synaptonemal complex. Chromosoma **115**, 175–194 (2006)
9. Cook, P.R.: The transcriptional basis of chromosome pairing. J. Cell Sci. **110**, 1033–1040 (1997)
10. Barzel, A., Kupiec, M.: Finding a match: how do homologous sequences get together for recombination? Nat. Rev., Genet. **9**, 27–37 (2008)
11. Zhou, H.X., Rivas, G., Minton, A.P.: Macromolecular crowding and confinement: biochemical, biophysical, and potential physiological consequences. Ann. Rev. Biophys. **37**, 375–397 (2008)
12. Kornyshev, A.A., Leikin, S.: Sequence recognition in the pairing of DNA duplexes. Phys. Rev. Lett. **86**, 3666–3669 (2001)
13. Cherstvy, A.G., Kornyshev, A.A., Leikin, S.: Torsional deformation of double helix in interaction and aggregation of DNA. J. Phys. Chem., B **108**, 6508–6518 (2004)
14. Kornyshev, A.A.: Physics of DNA: unravelling hidden abilities encoded in the structure of 'the most important molecule'. Phys. Chem. Chem. Phys. **12**, 12352–12378 (2010)
15. Baldwin, G.S., Brooks, N.J., Robson, R.E., Wynveen, A., Goldar, A., Leikin, S., Seddon, J.M., Kornyshev, A.A.: DNA double helices recognize mutual sequence homology in a protein free environment. J. Phys. Chem., B **112**, 1060–1064 (2008)
16. Danilowicz, C., Lee, C.H., Kim, K., Hatch, K., Coljee, V.W., Kleckner, N., Prentiss, M.: Single molecule detection of direct, homologous, DNA/DNA pairing. Proc. Natl. Acad. Sci. U. S. A. **106**, 19824–19829 (2009)
17. Cherstvy, A.G.: DNA-DNA sequence homology recognition: physical mechanisms and open questions. J. Mol. Recognit. **24**, 283–287 (2011)

18. Wiggins, P.A., Dame, R.T., Noom, M.C., Wuite, G.J.: Protein-mediated molecular bridging: a key mechanism in biopolymer organization. Biophys. J. **97**, 1997–2003 (2009)
19. Fudenberg, G., Mirny, L.A.: Higher-order chromatin structure: bridging physics and biology. Curr. Opin. Genet. Dev. **22**, 115–124 (2012)
20. Heermann, D.W., Jerabek, H., Liu, L., Li, Y.: A model for the 3D chromatin architecture of pro and eukaryotes. Methods, **58**, 307–314 (2012)
21. Handoko, L., Xu, H., Li, G., Ngan, C.Y., Chew, E., Schnapp, M., Lee, C.W., Ye, C., Ping, J.L., Mulawadi, F., Wong, E., Sheng, J., Zhang, Y., Poh, T., Chan, C.S., Kunarso, G., Shahab, A., Bourque, G., Cacheux-Rataboul, V., Sung, W.K., Ruan, Y., Wei, C.L.: CTCF-mediated functional chromatin interactome in pluripotent cells. Nat. Genet. **43**, 630–638 (2011)
22. Lieberman-Aiden, E., van Berkum, N.L., Williams, L., Imakaev, M., Ragoczy, T., Telling, A., Amit, I., Lajoie, B.R., Sabo, P.J., Dorschner, M.O., Sandstrom, R., Bernstein, B., Bender, M.A., Groudine, M., Gnirke, A., Stamatoyannopoulos, J., Mirny, L.A., Lander, E.S., Dekker, J.: Comprehensive mapping of long-range interactions reveals folding principles of the human genome. Science **326**(5950), 289–293 (2009)
23. Barbieri, M., Chotalia, M., Fraser, J., Lavitas, L.M., Dostie, J., Pombo, A., Nicodemi, M.: Complexity of chromatin folding is captured by the strings and binders switch model. Proc. Natl. Acad. Sci. U. S. A. **109**, 16173–16178 (2012)
24. Schiessel, H.: The physics of chromatin. J. Phys.: Cond. Matt. **15**, R699–R774 (2003)
25. Müller, K.P., Erdel, F., Caudron-Herger, M., Marth, C., Fodor, B.D., Richter, M., Scaranaro, M., Beaudouin, J., Wachsmuth, M., Rippe, K.: Multiscale analysis of dynamics and interactions of heterochromatin protein 1 by fluorescence fluctuation microscopy. Biophys. J. **97**, 2876–2885 (2009)
26. Boy de la Tour, E., Laemmli, U.K.: The metaphase scaffold is helically folded: sister chromatids have predominantly opposite helical handedness. Cell **55**, 937–944 (1988)
27. Joti, Y., Hikima, T., Nishino, Y., Kamada, F., Hihara, S., Takata, H., Ishikawa, T., Maeshima, K.: Chromosomes without a 30-nm chromatin fiber. Nucleus **3**, 1 (2012)
28. Woodcock, C.L., Skoultchi, A.I., Fan, Y.: Role of linker histone in chromatin structure and function: H1 stoichiometry and nucleosome repeat length. Chromos. Res. **14**, 17–25 (2006)
29. Potoyan, D.A., Papoian, G.A.: Regulation of the H4 tail binding and folding landscapes via Lys-16 acetylation. Proc. Natl. Acad. Sci. U. S. A. **109**, 17857–17862 (2012)
30. Li, G., Reinberg, D.: Chromatin higher-order structures and gene regulation. Curr. Opin. Genet. Dev. **21**, 175–186 (2011)
31. Poirier, M.G., Oh, E., Tims, H.S., Widom, J.: Dynamics and function of compact nucleosome arrays. Nat. Struct. Mol. Biol. **16**, 938–944 (2009)
32. Scheffer, M.P., Eltsov, M., Frangakis, A.S.: Evidence for short-range helical order in the 30-nm chromatin fibers of erythrocyte nuclei. Proc. Natl. Acad. Sci. U. S. A. **108**, 16992–16997 (2011)
33. Nishino, Y., Eltsov, M., Joti, Y., Ito, K., Takata, H., Takahashi, Y., Hihara, S., Frangakis, A.S., Imamoto, N., Ishikawa, T., Maeshima, K.: Human mitotic chromosomes consist predominantly of irregularly folded nucleosome fibres without a 30-nm chromatin structure. EMBO J. **31**, 1644–1653 (2012)
34. Depken, M., Schiessel, H.: Nucleosome shape dictates chromatin fiber structure. Biophys. J. **96**, 777–784 (2009)
35. Emanuel, M., Radja, N.H., Henriksson, A., Schiessel, H.: The physics behind the larger scale organization of DNA in eukaryotes. Phys. Biol. **6**, 025008 (2009)
36. Carrivain, P., Cournac, A., Lavelle, C., Lesne, A., Mozziconacci, J., Paillusson, F., Signon, L., Victor, J.-M., Barbi, M.: Electrostatics of DNA compaction in viruses, bacteria and eukaryotes: functional insights and evolutionary perspective. Soft Matter. **8**, 9285–9301 (2012)
37. Wedemann, G., Langowski, J.: Computer simulation of the 30-nanometer chromatin fiber. Biophys. J. **82**, 2847–2859 (2002)
38. Boroudjerdi, H., Naji, A., Netz, R.R.: Salt-modulated structure of polyelectrolyte-macroion complex fibers. Eur. Phys. J., E **34**, 72–90 (2011)
39. Kepper, N., Foethke, D., Stehr, R., Wedemann, G., Rippe, K.: Nucleosome geometry and internucleosomal interactions control the chromatin fiber conformation. Biophys. J. **95**, 3692–3705 (2008)
40. Schlick, T., Perisic, O.: Mesoscale simulations of two nucleosome-repeat length oligonucleosomes. Phys. Chem. Chem. Phys. **11**, 10729–10737 (2009)
41. Stolz, R.C., Bishop, T.C.: ICM Web: the interactive chromatin modeling web server. Nucl. Acids Res. **38**, W254–W261 (2010)
42. Voltz, K., Trylska, J., Calimet, N., Smith, J.C., Langowski, J.: Unwrapping of nucleosomal DNA ends: a multiscale molecular dynamics study. Biophys. J. **102**, 849–858 (2012)

43. Korolev, N., Allahverdi, A., Yang, Y., Fan, Y., Lyubartsev, A.P., Nordenskiöld, L.: Electrostatic origin of salt-induced nucleosome array compaction. Biophys. J. **99**, 1896–1905 (2010)
44. Korolev, N., Fan, Y., Lyubartsev, A.P., Nordenskiöld, L.: Modelling chromatin structure and dynamics: status and prospects. Curr. Opin. Struck. Biol. **22**, 151–159 (2012)
45. Korolev, N., Allahverdi, A., Lyubartsev, A.P., Nordenskiöld, L.: The polyelectrolyte properties of chromatin. Soft Matter. **8**, 9322–9333 (2012)
46. Finch, J.T., Klug, A.: Solenoidal model for superstructure in chromatin. Proc. Natl. Acad. Sci. U. S. A. **73**, 1897–1901 (1976)
47. Thoma, F., Koller, T., Klug, A.: Involvement of histone H1 in the organization of the nucleosome and of the saltdependent superstructures of chromatin. J. Cell. Biol. **83**, 403–427 (1979)
48. Cherstvy, A.G., Everaers, R.: Electrostatic interactions of DNA can quantize azimuthal orientations of nucleosome core particles in bilayers. J. Phys.: Cond. Mat. **18**, 11429–11442 (2006)
49. Kornyshev, A.A., Leikin, S.: Electrostatic zipper motif for DNA aggregation. Phys. Rev. Lett. **82**, 4138–4141 (1999)
50. Cherstvy, A.G.: Electrostatic interactions in biological DNA-related systems. Phys. Chem. Chem. Phys. **13**, 9942–9968 (2011)
51. Dekker, J., Rippe, K., Dekker, M., Kleckner, N.: Capturing chromosome conformation. Science **295**, 1306–1311 (2002)
52. Yaffe, E., Tanay, A.: Probabilistic modeling of Hi-C contact maps eliminates systematic biases to characterize global chromosomal architecture. Nat. Genet. **43**, 1059–1065 (2011)
53. Sexton, T., Yaffe, E., Kenigsberg, E., Bantignies, F., Leblanc, B., Hoichman, M., Parrinello, H., Tanay, A., Cavalli, G.: Three-dimensional folding and functional organization principles of the Drosophila genome. Cell **148**, 458–472 (2012)
54. Zhang, Y., McCord, R.P., Ho, Y.J., Lajoie, B.R., Hildebrand, D.G., Simon, A.C., Becker, M.S., Alt, F.W., Dekker, J.: Spatial organization of the mouse genome and its role in recurrent chromosomal translocations. Cell **148**, 908–921 (2012)
55. Cremer, T., Cremer, C.: Chromosome territories, nuclear architecture and gene regulation in mammalian cells. Nat. Rev., Genet. **2**, 292–301 (2001)
56. Cremer, T., Cremer, M.: Chromosome territories. Cold Spring Harbor Perspect. Biol. **2**, a003889 (2010)
57. Robinson, P.J.J., Fairall, L., Huynh, V.A.T., Rhodes, D.: EM measurements define the dimensions of the "30-nm" chromatin fiber: evidence for a compact, interdigitated structure. Proc. Natl. Acad. Sci. U. S. A. **103**, 6506–6511 (2006)
58. Routh, A., Sandin, S., Rhodes, D.: Nucleosome repeat length and linker histone stoichiometry determine chromatin fiber structure. Proc. Natl. Acad. Sci. U. S. A. **105**, 8872–8877 (2008)
59. Lanzani, G., Schiessel, H.: Out of register: how DNA determines the chromatin fiber geometry. Europhys. Lett. **97**, 38002 (2012)
60. Yager, T.D., McMurray, C.T., van Holde, K.E.: Salt-induced release of DNA from nucleosome core particles. Biochemistry **28**, 2271–2281 (1989)
61. Grigoryev, S.A., Arya, G., Correll, S., Woodcock, C.L., Schlick, T.: Evidence for heteromorphic chromatin fibers from analysis of nucleosome interactions. Proc. Natl. Acad. Sci. U. S. A. **106**, 13317–13322 (2009)
62. Woodcock, C., Ghosh, R.P.: Chromatin higher-order structure and dynamics. Cold Spring Harbor Perspect. Biol. **2**, a000596 (2010)
63. Kornyshev, A.A., Leikin, S.: Theory of interaction between helical molecules. J. Chem. Phys. **107**, 3656–3674 (1997)
64. Albini, S.M., Jones, G.H.: Synaptonemal complex spreading in *Allium cepa* and *A. fistulosum*. Chromosoma (Berl) **95**, 324–338 (1987)
65. Kornyshev, A.A., Lee, D.J., Leikin, S., Wynveen, A.: Structure and interactions of biological helices. Rev. Mod. Phys. **79**, 943–996 (2007)
66. Cherstvy, A.G.: Electrostatic of DNA complexes with cationic lipids. J. Phys. Chem., B **111**, 7914–7927 (2007)
67. Cherstvy, A.G.: Probing DNA-DNA electrostatic friction in tight superhelical DNA plies. J. Phys. Chem., B **113**, 5350–5355 (2009)
68. Cherstvy, A.G., Kornyshev, A.A.: DNA melting in aggregates: impeded or facilitated? J. Phys. Chem., B **109**, 13024–13029 (2005)
69. Lee, D.J., Wynveen, A., Kornyshev, A.A., Leikin, S.: Undulations enhance the effect of helical structure on DNA interactions. J. Phys. Chem., B **114**, 11668–11680 (2010)
70. Cherstvy, A.G.: DNA cholesteric phases: the role of DNA molecular chirality and DNA-DNA electrostatic interactions. J. Phys. Chem., B **112**, 12585–12595 (2008)

71. Cherstvy, A.G., Winkler, R.G.: Simple model for overcharging of a sphere by a wrapped oppositely charged asymmetrically neutralized polyelectrolyte: possible effects of helical charge distribution. J. Phys. Chem., B **109**, 2962–2969 (2005)
72. Andrews, A.J., Luger, K.: Nucleosome structure(s) and stability: variations on a theme. Annu. Rev. Biophys. **40**, 99–117 (2011)
73. Cherstvy, A.G.: Positively charged residues in DNA-binding domains of structural proteins follow sequence-specific positions of DNA phosphate groups. J. Phys. Chem., B **113**, 4242–4247 (2009)
74. Cherstvy, A.G.: PhD Thesis, "Interaction, recognition, and condensation of DNA duplexes". Düsseldorf University (2002)
75. Schlick, T., Hayes, J., Grigoryev, S.: Toward convergence of experimental studies and theoretical modeling of the chromatin fiber. J. Biol. Chem. **287**, 5183–5191 (2012)
76. Bednar, J., Dimitrov, S.: Chromatin under mechanical stress: from single 30 nm fibers to single nucleosomes. FEBS J. **278**, 2231–2243 (2011)
77. Lee, D.J.: Private communication
78. Segal, E., Fondufe-Mittendorf, Y., Chen, L., Thåström, A., Field, Y., Moore, I.K., Wang, J.P., Widom, J.: A genomic code for nucleosome positioning. Nature **442**, 772–778 (2006)
79. Lantermann, A.B., Straub, T., Strålfors, A., Yuan, G.C., Ekwall, K., Korber, P.: Schizosaccharomyces pombe genome-wide nucleosome mapping reveals positioning mechanisms distinct from those of Saccharomyces cerevisiae. Nat. Struct. Mol. Biol. **17**, 251–257 (2010)
80. Savić, A., Richman, P., Williamson, P., Poccia, D.: Alterations in chromatin structure during early sea urchin embryogenesis. Proc. Natl. Acad. Sci. U. S. A. **78**, 3706–3710 (1981)
81. Valouev, A., Johnson, S.M., Boyd, S.D., Smith, C.L., Fire, A.Z., Sidow, A.: Determinants of nucleosome organization in primary human cells. Nature **474**, 516–520 (2011)
82. Längst, G., Teif, V.B., Rippe, K.: Chromatin remodeling and nucleosome positioning. In: Rippe, K. (ed.) Genome Organization and Function in the Cell Nucleus, pp. 111–139. Wiley-VCH, Weinheim (2011)
83. Kornyshev, A.A., Leikin, S.: Symmetry laws for interaction between helical macromolecules. Biophys. J. **75**, 2513–2519 (1998)
84. Kornyshev, A.A., Leikin, S.: Electrostatic interaction between helical macromolecules in dense aggregates: an impetus for DNA poly- and meso-morphism. Proc. Natl. Acad. Sci. U. S. A. **95**, 13579–13584 (1998)
85. Saiz, L., Rubi, J.M., Vilar, J.M.: Inferring the in vivo looping properties of DNA. Proc. Natl. Acad. Sci. U. S. A. **102**, 17642–17645 (2005)
86. Rippe, K., von Hippel, P.H., Langowski, J.: Action at a distance: DNA-looping and initiation of transcription. Trends Biochem. Sci. **20**, 500–506 (1995)
87. Teif, V.B., Vainshtein, Y., Caudron-Herger, M., Mallm, J.-P., Marth, C., Höfer, T., Rippe, K.: Genome-wide nucleosome positioning during embryonic stem cell development. Nature Struct. Mol. Biol. **19**, 1185–1192 (2012)
88. Fu, Y., Sinha, M., Peterson, C.L., Weng, Z.: The insulator binding protein CTCF positions 20 nucleosomes around its binding sites across the human genome. PLoS Genetics **4**, e1000138 (2008)
89. Martin, D., Pantoja, C., Fernández, Miñán, A., Valdes-Quezada, C., Moltó, E., Matesanz, F., Bogdanovic, O., de la Calle-Mustienes, E., Domínguez, O., Taher, L., Furlan-Magaril, M., Alcina, A., Cañón, S., Fedetz, M., Blasco, M.A., Pereira, P.S., Ovcharenko, I., Recillas-Targa, F., Montoliu, L., Manzanares, M., Guigó, R., Serrano, M., Casares, F., Gómez-Skarmeta, J.L.: Genome-wide CTCF distribution in vertebrates defines equivalent sites that aid the identification of disease-associated genes. Nat. Struct. Mol. Biol. **18**, 708–714 (2011)
90. Ohlsson, R., Lobanenkov, V., Klenova, E.: Does CTCF mediate between nuclear organization and gene expression? BioEssays **32**, 37–50 (2010)
91. Borukhov, I., Lee, K.-C., Bruinsma, R.F., Gelbart, W.M., Liu, A.J., Stevens, M.J.: Association of two semiflexible polyelectrolytes by interchain linkers: theory and simulations. J. Chem. Phys. **117**, 462–480 (2002)
92. de Vries, R.: Influence of mobile DNA-protein-DNA bridges on DNA configurations: coarse-grained Monte-Carlo simulations. J. Chem. Phys. **135**, 125104 (2011)
93. Teif, V.B.: Ligand-induced DNA condensation: choosing the model. Biophys. J. **89**, 2574–2587 (2005)
94. Teif, V.B., Bohinc, K.: Condensed DNA: condensing the concepts. Prog. Biophys. Mol. Biol. **105**, 208–222 (2011)
95. Nicodemi, M., Panning, B., Prisco A.: A thermodynamic switch for chromosome colocalization. Genetics **179**, 717–721 (2008)
96. Scialdone, A., Nicodemi, M.: Diffusion-based DNA target colocalization by thermodynamic mechanisms. Development **137**, 3877–3885 (2010)

97. Cherstvy, A.G., Kolomeisky, A.A., Kornyshev, A.A.: Protein-DNA interactions: reaching and recognizing the targets. J. Phys. Chem., B **112**, 4741–4750 (2008)
98. Kontorova, T.A., Frenkel, YaI.: On the theory of plastic deformation and twinning I. Zh. Eksp. Teor. Fiz. **8**, 89 (1938)
99. Braun, O.M., Kivshar, Y.S.: Nonlinear dynamics of the Frenkel-Kontorova model. Phys. Rep. **306**, 1–108 (1998)
100. Kornyshev, A.A., Wynveen, A.: Nonlinear effects in the torsional adjustment of interacting DNA. Phys. Rev., E **69**, 041905 (2004)
101. Bancaud, A., Huet, S., Daigle, N., Mozziconacci, J., Beaudouin, J., Ellenberg, J.: Molecular crowding affects diffusion and binding of nuclear proteins in heterochromatin and reveals the fractal organization of chromatin. EMBO J. **28**, 3785–3798 (2009)
102. Leikin, S., Parsegian, V.A.: Temperature-induced complementarity as a mechanism for biomolecular assembly. Proteins **19**, 73–76 (1994)
103. Milla, M., Daban, J.R.: Self-assembly of thin plates from micrococcal nuclease-digested chromatin of metaphase chromosomes. Biophys. J. **103**, 567–575 (2012)
104. Zimmerman, S.B., Minton, A.P.: Macromolecular crowding: biochemical, biophysical, and physiological consequences. Annu. Rev. Biophys. Biomol. Struct. **22**, 27–65 (1993)
105. Zhou, H.X.: Protein folding and binding in confined spaces and in crowded solutions. J. Mol. Recognit. **17**, 368–375 (2004)
106. Sereshki, L.E., Lomholt, M.A., Metzler, R.: A solution to the subdiffusion-efficiency paradox: inactive states enhance reaction efficiency at subdiffusion conditions in living cells. Europhys. Lett. **97**, 20008 (2012)
107. Cortini, R., Kornyshev, A.A., Lee, D.J., Leikin, S.: Electrostatic braiding and homologous pairing of DNA double helices. Biophys. J. **101**, 875–884 (2011)
108. Barkai, E., Garini, Y., Metzler, R.: Strange kinetics of single molecules in living cells. Phys. Today **65**, 29–35 (2012)
109. Rosa, A., Everaers, R.: Structure and dynamics of interphase chromosomes. PLoS Comput. Biol. **4**, e1000153 (2008)
110. Winkler, R.G., Cherstvy, A.G.: Strong and weak polyelectrolyte adsorption onto oppositely charged curved surfaces. Adv. Polym. Sci. doi:10.1007/12_2012_183(2013)
111. Wong, H., Victor, J.-M., Mozziconacci, J.: An all-atom model of the chromatin fiber containing linker histones reveals a versatile structure tuned by the nucleosomal repeat length. PLos ONE **2**, e877 (2007)
112. Chua, E.Y.D., Vasudevan, D., Davey, G.E., Wu, B., Davey, C.A.: The mechanics behind DNA sequence-dependent properties of the nucleosome. Nucl. Acids Res. **40**, 6338–6352 (2012)
113. Nishikawa, J., Ohyama, T.: Selective association between nucleosomes with identical DNA sequences. Nucl. Acids Res. (2013). doi:10.1093/nar/gks1269